

Modeling interacting dynamic networks: II. Systematic study of the statistical properties of cross-links between two networks with preferred degrees

Wenjia Liu¹, B. Schmittmann^{1,2}, and R. K. P. Zia^{1,2}

¹Department of Physics and Astronomy, Iowa State University, Ames, IA 50011, USA

²Department of Physics, Virginia Tech, Blacksburg, VA 24061

E-mail: wjliu@iastate.edu, schmittb@iastate.edu and rkpzia@vt.edu

Abstract. In a recent work [1], we introduced dynamic networks with preferred degrees and presented simulation and analytic studies of a single, homogeneous system as well as two interacting networks. Here, we extend these studies to a wider range of parameter space, in a more systematic fashion. Though the interaction we introduced seems simple and intuitive, it produced dramatically different behavior in the single- and two-network systems. Specifically, partitioning the single network into two identical sectors, we find the cross-link distribution to be a sharply peaked Gaussian. In stark contrast, we find a very broad and flat plateau in the case of two interacting identical networks. A sound understanding of this phenomenon remains elusive. Exploring more asymmetric interacting networks, we discover a kind of ‘universal behavior’ for systems in which the ‘introverts’ (nodes with smaller preferred degree) are far outnumbered. Remarkably, an approximation scheme for their degree distribution can be formulated, leading to very successful predictions.

1. INTRODUCTION

Complex networks can be found everywhere in our world, ranging from neuronal architectures to galactic filaments and from facebook to transportation systems [2, 3, 4, 5, 6]. To understand the behavior of these systems requires both powerful analytic tools and access to large data sets. Thanks to the rapid pace of development in information technology, considerable amount of data can be collected and systematic descriptions of various features of these systems have been initiated. At the same time, an interdisciplinary academic field – network science – has become quite mature, establishing a powerful framework for characterizing and analyzing complex networks, as well as applying network representations successfully to study physical, biological, and infrastructure systems. In this context, early studies focus mainly on *static* networks, and are quite adequate for describing networks such as power grids and highways, whose topology can be regarded as constant (within the time scales of interest). However, in many other situations, such as social networks, a *dynamic* description would be more appropriate. Yet, there are far fewer studies for such networks. Recent and notable examples include the time evolution of network topology [7, 8, 9], dynamical processes on networks [10, 11], as well as the combination of both, namely, adaptive co-evolutionary networks [12, 13]. Within the physics community, most of these studies have focused on single isolated networks, putting aside the fact that real world systems are highly interconnected and therefore should be modelled as interacting networks. For instance, smartphones can help drivers avoid heavy traffic. This situation cannot be fully described in terms of a single network, whether we focus on cellular communication or the transportation (road) network. Therefore, models with interdependent networks are needed, culminating perhaps, in a ‘theory of networks of networks.’ In recent years, the significance of interdependent networks has begun to attract attention, and some aspects of such networks have been probed. Those studies include the investigation of critical infrastructure interdependencies [14, 15, 16, 17, 18], and approaches such as the multilayer method to couple traffic flows to physical infrastructures [19].

While our ultimate goal is to understand the interdependence of dynamic networks, we begin with simple model systems, in order to gain some insight into the effects of interactions. In particular, we focus on networks with ‘preferred degrees,’ which allow us to implement both dynamics and interactions easily. In the first paper of this series [1], we introduced such a dynamic network, in which each node is pre-assigned a preferred degree (κ) and, when chosen to act, adds/cuts links to reach and maintain κ . Since the dynamics does not obey detailed balance in general, these systems settle eventually into *non-equilibrium steady states* (in contrast to systems in thermal equilibrium controlled by Boltzmann weights). In our studies here, we devote attention solely to such states. We first consider a homogeneous population and discover some unexpected properties of this network. Then, we introduce a coupling between two such networks and investigate the effects of their interaction. In [1], we focused predominantly on various degree distributions and found that they differ significantly from the Poisson in a standard

Erdős-Rényi random network [20]. Within the limited range of parameter space studied there, the degree distributions ($\rho(k)$'s) can be reasonably explained by a mean-field approach. For a few special choices of parameters, we already noted that the interaction between just two populations can induce highly non-trivial behavior of X , the total number of cross-links between them. In this paper, we probe the parameter space more systematically, focusing specifically on the properties of the mean, $\langle X \rangle$, and standard deviation, σ_X . In some special cases, we delve into more detail, such as various degree distributions in the steady state ($\rho^{ss}(k)$), as well as the distribution for the cross-links: $P^{ss}(X)$. For a homogeneous population, by defining X to be the total number of cross-links between two identical partitions, we find the stationary distribution $P^{ss}(X)$ to be a narrowly peaked distribution, well described by a Gaussian. By contrast, for a very similar two-network model, which we refer to as the ‘symmetric system,’ $P^{ss}(X)$ displays a broad and flat plateau! Moreover, the power spectrum of $X(t)$ shows that the dynamics of X is consistent with an *unbiased* random walk (within some bounds). The dramatic difference between such similar models illustrates that the non-trivial behavior of X is indeed a consequence of the interaction between networks.

The remainder of this paper is organized as follows. In Section 2, we present the specifications of our models and introduce several quantities that serve to describe the topology of our networks. In Section 3, we show the Monte Carlo simulation results along with some analytical understandings. In the last Section, we provide a summary and outlook for this paper.

2. SPECIFICATIONS OF THE MODELS

2.1. A single network with a preferred degree (single-network model)

Recently, we introduced a class of dynamic networks evolving according to one or more preferred degrees [21, 22, 23, 24, 1]. The motivation of such a model lies with the belief that, in typical social settings, an individual would *prefer* to have a certain number of contacts. For example, an introvert may prefer only a handful of friends, while an extrovert would be glad to have hundreds or thousands of contacts. Of course, real social interactions are far more complex, and so we use the notion of ‘extroverts’ and ‘introverts’ only as an illustration. For the readers’ convenience, we briefly summarize the main features of our model here.

In the simplest case, we model a homogeneous population of N nodes (individuals), all assigned the same ‘preferred degree,’ κ . When chosen for updates, a node will attempt to add or cut one of its links based on κ . In each attempt, a node is randomly chosen, its degree (k) is noted, and depending on whether k is smaller/larger than κ , k will be increased/decreased by one. (To avoid ambiguity, κ is always chosen to be slightly larger than the integer quoted, e.g., $\kappa = 25$ really means 25.5. Here, this step is deterministic, while stochastic rules can be implemented [22, 1].) In this sense, a node ‘prefers’ to have degree κ . For simplicity, the action of adding/cutting is performed on a randomly

chosen partner which has no/a link with the node. The partner node is passive and has no influence on this action. Self-loops and multiple connections are not allowed. In our simulation, one Monte Carlo step (MCS) consists of N such attempts, so that, on the average, each node has one chance to take action. Clearly, the network is dynamic, while the node attributes remain static. At large times, the system will reach a steady state, with statistically stationary network topology. Not surprisingly, the average degree is κ . However, despite the appearance of randomness, the degree distribution is neither Poisson nor Gaussian, but Laplacian [1].

2.2. Modelling the interaction between two networks (two-network model)

Our goal is to study interactions between two such networks, with different κ 's and N 's in general. One quantity of interest is X , the total number of cross-links between the two networks. X is clearly a quantitative measure of the interaction between them. Next, let us introduce the 'interactions.' Of course, there are infinitely many ways to do so and we can explore only a few, motivated by what seems the most likely behavior between individuals in two populations. In this paper, we begin with arguably the simplest: χ , the probability a node acts (add or cut) on a cross-link. A few other forms of natural 'interactions' will be considered in the last paper of this series.

Consider two preferred degree networks (labelled by $\alpha = 1, 2$), with N_α nodes, preferred degrees κ_α , and cross-link action χ_α . In each attempt, one node is chosen at random from all the N ($= N_1 + N_2$) nodes. If the degree of this node is lower/higher than κ_α , it will attempt to add/cut a link. With probability χ_α , this action will be taken with a partner node from the *other* network. Thus, an intra-community link will be updated with probability $1 - \chi_\alpha$. In all cases, the partner node will be randomly picked from the chosen group. If a suitable partner does not exist (e.g., when the action is to cut and there are no links to nodes in the chosen community), then no action is taken. As usual, one MCS involves N such attempts. In all our simulations, the initial network is entirely devoid of links, i.e., a null graph.

With this set-up, the parameters χ_α clearly control the behavior of X . In the extreme case of $\chi_\alpha = 0$, $X \equiv 0$ as the two networks decouple completely. At the other extreme, $\chi_\alpha = 1$, the system consists of only bipartite graphs, though not a complete one in general ($X < N_1 N_2$). With only cross-links, such a system may be regarded as 'fully interacting.' In this sense, χ plays the role of an interaction strength.

2.3. Quantities of interest

One of the standard characterizations of the topology of a network is the degree distribution, $\rho(k)$. Denoting by n_k the number of nodes with k links in each measurement, $\rho(k)$ is given by

$$\rho(k) = \frac{\langle n_k \rangle}{N}. \quad (1)$$

For a homogeneous network with a single preferred degree, this ρ is, as expected, sharply peaked around κ . In a system with two sub-networks with different preferred degrees, it is expected to be bimodal, especially if the κ 's are far apart. Thus, it is sensible to consider separate distributions, $\rho_\alpha(k)$, associated with nodes in community α which have degree k . Beyond these, we may extend our considerations to the next level of detail, $\rho_{\alpha\beta}(k_{\alpha\beta})$, associated with $k_{\alpha\beta}$, denoting the number of links with which a node in community α is connected to nodes in community β . Note that $\langle k_{12} \rangle \neq \langle k_{21} \rangle$, since the average number of cross-links $\langle X \rangle$ is equal to both $N_1 \langle k_{12} \rangle$ and $N_2 \langle k_{21} \rangle$. Though somewhat cumbersome (compared to $\rho_{\alpha\beta}(k)$), we will use the notation above, to leave no doubt about which quantity is being considered. We will also refer to ρ_α as a 'global degree distribution,' reserving the terms internal/external degree distribution for $\rho_{\alpha\alpha} / \rho_{\alpha\beta}$. Our study will be mainly for the steady state, for which we add the superscript *ss*, e.g., ρ_{12}^{ss} .

Of course, we can proceed further and consider joint distributions, such as $P_1(k_{11}, k_{12})$, the probability that a node in community 1 will be found with degrees k_{11} and k_{12} , etc. For this paper, however, we will limit ourselves to the less detailed distributions. Clearly,

$$\rho_\alpha(k) \equiv \sum_{k_{\alpha\alpha}, k_{\alpha\beta}} \delta(k_{\alpha\alpha} + k_{\alpha\beta} - k) P_\alpha(k_{\alpha\alpha}, k_{\alpha\beta}) \quad (2)$$

while $\rho_{\alpha\alpha}$ and $\rho_{\alpha\beta}$ are simple projections of P_α , e.g., $\rho_{\alpha\alpha}(k_{\alpha\alpha}) = \sum_{k_{\alpha\beta}} P_\alpha(k_{\alpha\alpha}, k_{\alpha\beta})$. These remarks show that ρ_α , e.g., cannot be obtained from $\rho_{\alpha\alpha}$ and $\rho_{\alpha\beta}$ in general.

As we are interested in the behavior of the cross-network interactions, most of our attention will be on cross-links. While much information is stored in $\rho_{\alpha\beta}$, it is more efficient to study the 'macroscopic' quantity, X , specifically its mean, $\langle X \rangle$, and standard deviation, σ_X . For a special case (see Eqn. (3) below), its time dependence in the steady state will be analyzed in more detail. Thus, $X(t)$ will be used to compile a histogram which represents $P^{ss}(X)$, while its power spectrum will be exploited to reveal the nature of the dynamics leading to P^{ss} . In particular, a surprising discovery is that, under certain conditions, X performs an unbiased random walk over an extremely large fraction of its available range, so that P^{ss} displays a broad plateau instead of a sharp peak.

To determine which aspects of the interaction are crucial for the emergence of such remarkable phenomena, we compare two very similar systems. One is a homogeneous network of $2L$ nodes with κ . Arbitrarily labelling half of them as 'red' and the rest 'blue,' we mimic having two communities and define X as the total number of 'red-blue' links. The other system is the 'symmetric' two-network model:

$$N_1 = N_2 = L; \quad \kappa_1 = \kappa_2 = \kappa; \quad \chi_1 = \chi_2 = 0.5 \quad (3)$$

The apparent symmetry between the two communities may lead us to expect that the behavior of X in this system should be similar to that in the homogeneous population.

As will be shown in the next Section, this naive expectation is far from fulfilled and the simple interaction associated with χ has a profound effect on the macroscopic X .

Finally, in a social network with introverts and extroverts, ‘frustration’ is unavoidable. Instead of a qualitative notion, ‘frustration’ can be quantified in our model. For example, consider $\kappa_1 \ll \kappa_2$. Since a node plays a passive role for much of the time (as other individuals add/cut links to it), we should expect an introvert/extrovert (characterized by $\kappa_{1,2}$) to find itself mostly with more/less contacts than it prefers. In the steady state, we may define ‘frustration’ for *individual* i by

$$\phi_i \equiv \sum_{k>\kappa} \rho^{(i)}(k) - \sum_{k<\kappa} \rho^{(i)}(k) \quad (4)$$

where $\rho^{(i)}(k)$ is the degree distribution of i alone (and not of the population as a whole). With $\phi \in [-1, 1]$, its magnitude is a measure of how frustrated i is, while the sign provides its propensity to add/cut in its attempt to seek relief. Although we will not study this quantity in detail, we will use the concept in later discussions. Specifically, in the third paper of this series [26], we will investigate a ‘maximally frustrated’ population of extreme introverts ($\kappa_1 = 0_-$) and extroverts ($\kappa_2 = \infty$). Preliminary results of this system, reported elsewhere [24], showed the existence of a sharp transition in X when $N_1 - N_2$ changes sign.

3. SIMULATION RESULTS AND THEORETICAL CONSIDERATIONS

In general, there are three pairs of relevant control parameters when coupling two preferred degree networks with χ , namely, $N_{1,2}$, $\kappa_{1,2}$, and $\chi_{1,2}$. Exploring such a 6-dimensional space is beyond the scope of our study. We content ourselves with a limited region in certain subspaces, as most of our simulations focus on $N_1 + N_2 = 200$, $\kappa_1 + \kappa_2 = 50$, and $\chi_1 + \chi_2 = 1$. In particular, we begin with a symmetric system, Eqn. (3), and contrast its behavior to that in a homogeneous network with $N = 200$ and $\kappa = 25$. For more general cases, we reported results for systems with only one of the three pairs being different (i.e., along certain 1-d subspaces) [1]. Here, we extend our studies to certain 2-d subspaces, with two pairs of control parameters being distinct. Though an overall understanding of the behavior of these networks remains beyond our grasp, we are able to gain some insight, through a mean-field treatment, into systems where one community is ‘fully frustrated.’

3.1. Homogeneous vs. symmetric heterogeneous populations

A good baseline study of an interacting two-network system is the symmetric case. Specifically, we performed simulations mostly with $N_1 = N_2 = 100$, $\kappa_1 = \kappa_2 = 25$, and $\chi_1 = \chi_2 = 0.5$. Before we proceed to the results, let us recapitulate, for comparison, what is known about a very similar system consisting of just one homogeneous network ($N = 200$, $\kappa = 25$). Though we find an expected result – both systems displaying the

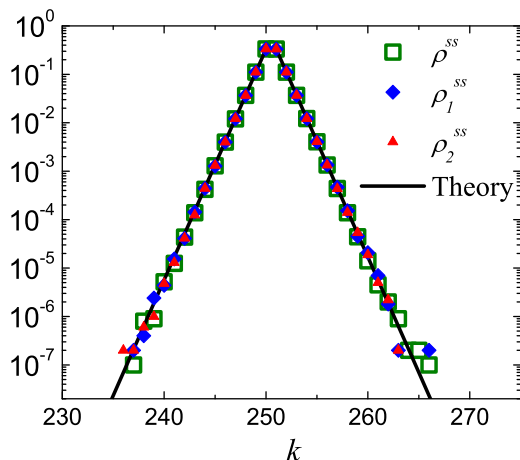


Figure 1. Degree distribution, ρ^{ss} , of a single network with $N = 1000$ and $\kappa = 250$ (green squares), along with the theoretical prediction (solid black line). For a system with two interacting networks, the total degree distributions are ρ_1^{ss} (blue diamonds) and ρ_2^{ss} (red triangles).

same degree distribution, $\rho^{ss}(k)$, we also discover a surprising one – drastically different behavior in X .

3.1.1. Steady state global degree distributions For the homogeneous population in the steady state, there is only one $\rho^{ss}(k)$, since all links are connected to nodes in the same network. Of all the distributions introduced above for two interacting networks, the most appropriate ones for this comparative study is the global distribution, ρ_1^{ss} , which should be same as ρ_2^{ss} for this symmetric case. As we found, these quantities settle down quite rapidly, so that we were able to exploit the relatively large systems ($L = 1000$ and $\kappa = 250$) used in previous studies [1]. Starting with empty networks, we discard the first $1K/2K$ MCS for the single-/two-network model. Thereafter, we measure the quantities of interest every 100 MCS and compile the average over 10^4 measurements. The resultant ρ^{ss} 's are shown in Fig. 1. It is clear that there is no discernible difference between all three distributions, as might be expected. For the reader's convenience, we recapitulate known properties of ρ^{ss} and how its form (neither Poisson nor Gaussian) can be understood [1]. We see that $\rho^{ss} \propto e^{-\mu|k-\kappa|}$ is a double exponential, i.e., a Laplacian. Our data indicate $\mu = 1.08 \pm 0.01$, which can be explained using a crude mean-field approximation to estimate the rates for our node to gain or lose a link. Respectively, these are $\Theta(\kappa - k) + 1/2$ and $\Theta(k - \kappa) + 1/2$, where Θ is the Heavyside function. The Θ terms correspond to how a chosen node will act, while the $1/2$ accounts for how its partner nodes will act. In the steady state, each node is 'content' on the average, and so, the probability to add/cut is just $1/2$. Balancing the gain/lose probability currents, we arrive at

$$\frac{\rho^{ss}(k+1)}{\rho^{ss}(k)} = \frac{\Theta(\kappa - k) + 1/2}{\Theta(k + 1 - \kappa) + 1/2} \quad (5)$$

which leads to $\rho^{ss}(k) \propto 3^{-|k-\kappa|}$, in excellent agreement with the data.

Needless to say, the same argument can be advanced for the *symmetric* two-network system, arriving at a similar result. However, as presented below, drastic differences between the single-network and the interacting networks emerge when we measure another quantity: X .

3.1.2. Behavior of the total number of cross-links, X In a previous paper [1], we investigated this quantity briefly. In particular, we found that $X(t)$ displays very large fluctuations and, for systems with $L = 1000$, it takes very long times ($\gg 3 \times 10^6$ MCS) for X to reach the limits of its range. To build reliable histograms, it would take even longer to collect enough data. Thus, we consider smaller systems for the remainder of this paper, namely, $L = 100$ and $\kappa = 25$. We also discard the initial 10^7 MCS, to let the system reach steady state, before taking measurements every 100 MCS for the next 2×10^7 MCS. With the resultant time trace of 2×10^5 points, we compile a histogram, which leads to $P^{ss}(X)$. We also construct a power spectrum. Specifically, we divide the entire time trace into 20 shorter ($10^4 \equiv T$) ones and obtain Fourier transformations of each: $\tilde{X}(\omega) \equiv \sum_{t=1}^T X(t)e^{i\omega t}$ where $\omega = 2\pi m/T$ ($m \in [0, T-1]$). The power spectrum, $I(\omega)$, is defined as the average $\langle |\tilde{X}(\omega)|^2 \rangle$ over these 20 FT's.

The results are plotted (in red) in Figs. 2 and 3. The presence of a broad plateau in $P^{ss}(X)$ motivates us to explore the dynamics of $X(t)$, to see if it simply performs an unbiased random walk within the confines of two ‘soft walls.’ This conjecture is confirmed by the latter plot, in which we see that $I(\omega)$ indeed follows $1/\omega^2$ quite well, crossing over (for small ω) to a constant dictated by the limits of X , namely, 0 and L^2 .

In stark contrast, the data displayed in green are indicative of very different behavior. Let us emphasize what X is – in this homogeneous population of 200 nodes, all preferring degree 25. First, we randomly partition the system into 2 sets of 100 nodes, labelling one set ‘blue’ and the other ‘red.’ At any t , the total number of ‘red-blue’ links is defined as X . Clearly, if we focus on any one node, there can be up to 199 contacts, though κ will limit the average to about 25.5. Thanks to homogeneity and the randomness in the dynamics, we can expect half of these to be cross-links. Thus, we are not surprised by the peak of $P^{ss}(X)$ being located at $\sim 100 \times 25.5/2 = 1275$. We can go further, to estimate the observed standard deviation ($\sigma_X \sim 25$) by the following crude argument. Denoting by x the number of cross-links of any node, we already arrived at its mean, i.e., $\langle x \rangle = 12.75$. If we assume that the distribution of x is a binomial distribution (with probability 1/2 that the node acts on a cross-link), then this standard deviation is, roughly, $\sigma_x = \sqrt{25.5/4}$. Invoking the central limit theorem for 100 nodes, we easily find $\sigma_X = \sqrt{100}\sigma_x \simeq 25$, in excellent agreement with observation. As for its dynamics, we expect $X(t)$ to be governed by white noise, as confirmed by the green line in Fig. 3.

By contrast, σ_X for the symmetric two-network system is over an order of magnitude larger: $\sim 300!$ (Of course, by symmetry, the average $\langle X \rangle$ is expected to be the similar, i.e., ~ 1250 .) The reason behind the failure of crude arguments for the symmetric, interacting two-network system is quite subtle. Exploring this non-trivial issue will be

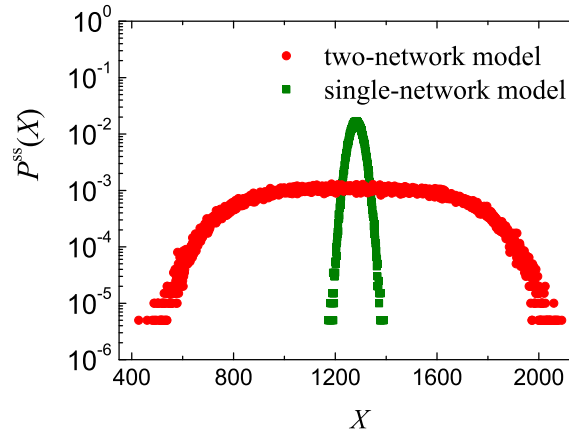


Figure 2. Comparison of histograms for the number of cross-links X : from a single, homogeneous network with $N = 200$, arbitrarily partitioned into two identical sections (green), and from a model with two interacting networks with $N_1 = N_2 = 100$ and $\chi_1 = \chi_2 = 0.5$ (red). In all cases, the preferred degree, κ , is 25.

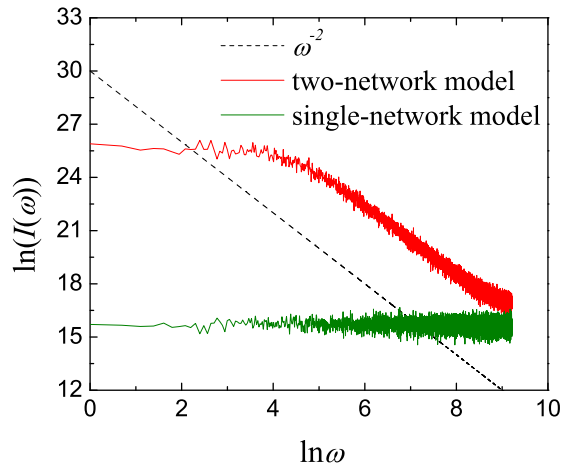


Figure 3. Power spectra, $I(\omega)$, associated with $X(t)$ for the two systems described in the caption of Fig. 2: green for the homogeneous network and red for the interacting two-network model.

the topic of the third paper in the series [26]. There, we will study the opposite (indeed, extreme) limit of this system, thereby bringing the essence of this remarkable behavior into sharp focus. For the remainder of this paper, we will report on more systematic studies of X in typical asymmetric two-network models.

3.2. Asymmetric heterogeneous populations

In this subsection, we venture from the special symmetric system and explore systematically a larger region of the 6-d parameter space: $(N_\alpha, \kappa_\alpha, \chi_\alpha)$. As a result,

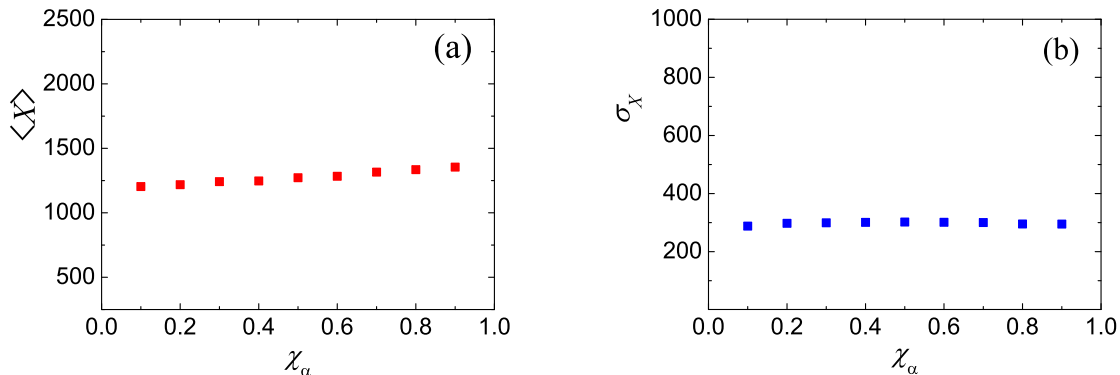


Figure 4. The means (red squares) and standard deviations (blue squares) associated with cross-links in a two-network model with $N_\alpha = 100$ and $\kappa_\alpha = 25$, as a function of $\chi_\alpha = \chi_1 = \chi_2$.

we will be unable to study details like the full $P^{ss}(X)$ or $I(\omega)$. Instead, we will show results on just the mean, $\langle X \rangle$, and the standard deviation, σ_X .[‡] To orient the reader in this space, we start from the specific case above ($N_\alpha = 100$, $\kappa_\alpha = 25$, $\chi_\alpha = 0.5$) and first extend along the 1-d lines by varying just one of these pairs, but keeping their values equal. While it is fair to refer to, say, a system with $\chi_1 = \chi_2 = 0.9$ as asymmetric (since the individuals do not choose intra-community partners with the same probability as cross-links), the other two ‘axes’ represent genuinely symmetric systems. Those studies (varying N_α or κ_α alone) should be regarded as explorations of the effects of population size and degree preference. In all these simulations, we again start with empty systems and carry out two independent runs, each 10^7 MCS long. X is measured once every 100 MCS, so that, for each case, there are 2×10^5 data points from which we compute the mean and standard deviation: $\langle X \rangle$, σ_X .

3.2.1. Results from varying one pair of parameters. We begin by varying $\chi_1 = \chi_2 = \chi$, with N_α and κ_α kept at 100 and 25, respectively. Recall that χ controls effectively the interaction between two networks, since individuals with larger χ are more likely to take action on cross-links. Thus, $\chi = 0$ represent two independent networks, while only cross-links are present in $\chi = 1$ networks. For general χ , however, it is not directly related to the value of X (but only to the likelihood for X to change). Therefore, our expectation is that changing χ would not affect $\langle X \rangle$ or σ_X . Fig. 4 shows the simulation results for $\chi = 0.1, \dots, 0.9$. Our expectation is largely borne out, especially for σ_X . There appears to be a slight rising trend in $\langle X \rangle$, $\sim 15\%$ over this entire range of χ . It is difficult to explain these variations in detail, though the typical values deviate little from that in the symmetric case ($\chi = 0.5$; $\langle X \rangle \sim 1272$), as predicted above. We will next see that more interesting behavior appears when we vary the other two control parameters.

[‡] In our previous study [1], we considered only a few specific points in this large parameter space. Thus, we were able to investigate more detailed properties, such as the four $\rho_{\alpha\beta}$ ’s.

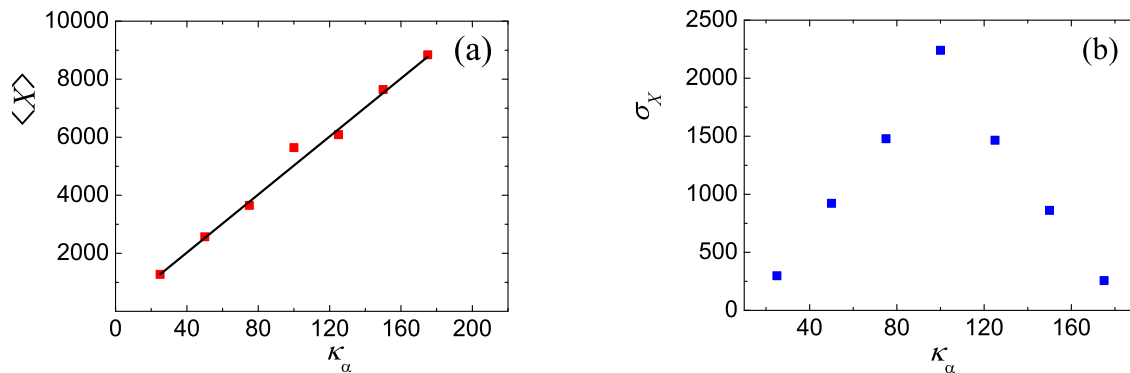


Figure 5. The means (red squares) and standard deviations (blue squares) associated with cross-links in a two-network model with $N_\alpha = 100$ and $\chi_\alpha = 0.5$, as a function of $\kappa_\alpha = \kappa_1 = \kappa_2$. In (a), $N_\alpha \kappa_\alpha / 2$ is also plotted (solid line) for comparison.

The next pair we vary is $\kappa_1 = \kappa_2 = \kappa$, with fixed $N_\alpha = L = 100$ and $\chi_\alpha = \chi = 0.5$. Fig. 5 shows the simulation results for $\kappa = 25, 50, 75, \dots, 175$. Needless to say, if κ exceeds the total population size, (200 in simulations here), every link will be established quickly, and X will be a constant $L^2 = 10^4$ and $\sigma_X \equiv 0$. Thus, our simulations sample essentially the entire range of meaningful κ 's here. Now, κ controls the preferred degree of a node and so, it is not surprising that $\langle X \rangle \propto \kappa$. In particular, since $\rho_\alpha(k)$ is sharply peaked at κ_α , a simple minded estimate is that each node has $\kappa_\alpha \chi_\alpha$ cross-links. Thus, we arrive at $\langle X \rangle \simeq \kappa_\alpha N_\alpha / 2$ ($= 50\kappa$ here), plotted as a solid line in Fig. 5 and in surprisingly good agreement with the data. We are unable to find a similar estimate for the behavior of σ_X . The most striking features there are: (i) σ_X varies linearly with κ and (ii) σ_X is symmetric around its peaks at 100. That σ_X vanishes at both end points is clear, but it is unclear how other features arise. A phenomenological formula which accounts for these features is $\sigma_X \propto \min(\langle X \rangle, L^2 - \langle X \rangle)$, but how it emerges from the underlying dynamics is unknown. In stark contrast, since this system is also ‘symmetric,’ an argument similar to the above (for its counterpart in a homogeneous population) would provide $\sqrt{N\kappa/4} = \sqrt{25\kappa}$, which clearly fails to match the data. Understanding the properties of σ_X here remains a challenge.

Finally, we vary $L = N_1 = N_2$ while holding $\kappa_\alpha = \kappa = 25$ and $\chi_\alpha = \chi = 0.5$. Due to limited computing power, we only explored an order of magnitude around 100: $L \in [50, 500]$, the results of which are shown in Fig. 6. Again, the dependence of the mean, $\langle X \rangle$, is easy to understand, namely, $\kappa \chi L \simeq 12.5L$ (solid line). However, similar to the systems reported above, the behavior of σ_X is more intriguing. In an inset of Fig. 6(b), we show a log-log plot of $\sigma_X - L$ and see that σ_X scales well as $L^{0.63}$. Such anomalous scaling hints at critical phenomena and deserves a thorough investigation. In particular, the incidence matrix associated with the two communities can be viewed as an $L \times L$ Ising model (in the lattice gas language, with 0, 1 in the entries). Then, X maps into $2M - L^2$, with M being the total magnetization, while the variance σ_X^2 corresponds to the Ising susceptibility ($\times L^2$). So, our findings here

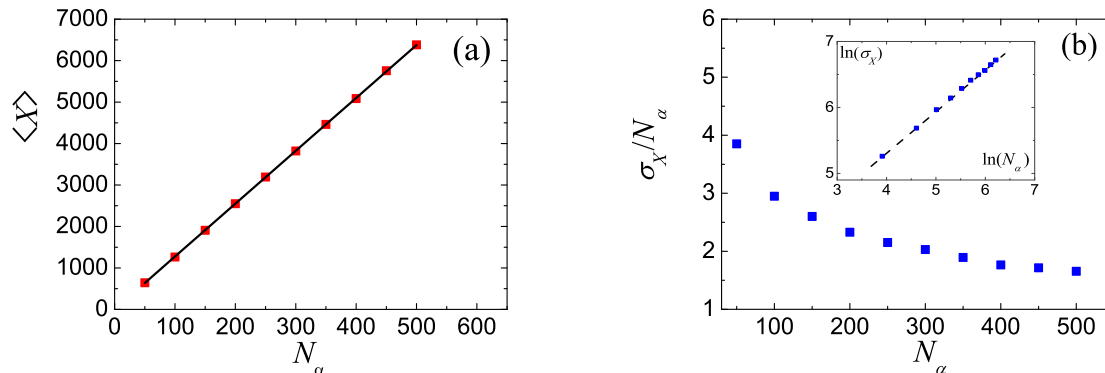


Figure 6. The means (red squares) and standard deviations (blue squares) associated with cross-links in a two-network model with $\kappa_\alpha = 25$ and $\chi_\alpha = 0.5$, as a function of $N_\alpha = N_1 = N_2$. In (a), $N_\alpha \kappa_\alpha / 2$ is also plotted (solid line) for comparison. The inset in (b) shows a log-log plot for σ_α (blue squares) as a function of N_α . For comparison, the dashed line reflects a power law, $\propto N_\alpha^{0.63}$.

imply a *decreasing* ‘susceptibility’ ($\sim L^{-0.74}$). This remarkable property can be argued qualitatively, as follow. Note that $\kappa\chi$ controls the creation of a cross-link, so that any particular link occurs, roughly, with probability $\kappa\chi/L$. Thus, increasing L while holding $\kappa\chi$ fixed corresponds to an increasingly stronger magnetic field, which in turn, leads to a decreasing magnetic susceptibility. In the next paper of this series [26], such a mapping can be established analytically (for the two-population model with maximally opposite preferences), while a system with $N_1 = N_2$ can be interpreted as a peculiar critical point [24].

3.2.2. Results from varying N_α and κ_α . In the previous subsection, we explored the region around a special symmetric two-network system by varying one pair of parameters (i.e., along certain lines). Here we turn our attention to a more general case, in which the networks differ by two parameters, specifically, just the sizes and the preferences. To make comparisons with the previously studied systems, we restrict ourselves to systems with fixed sums: $N_1 + N_2 = 200$, $\kappa_1 + \kappa_2 = 50$, and $\chi_1 + \chi_2 = 1$. Moreover, from the results above (especially Fig. 4), we see that the effects of changing χ are minimal. Thus, we simply fix both χ ’s to 0.5. As we vary N_α , over the entire range, we need to keep, say, only $\kappa_1 \leq \kappa_2$ to access the whole subspace of interest. This choice allows us to refer to $\alpha = 1, 2$ as the introverts and extroverts, respectively. In Fig. 7, we provide results for $\langle X \rangle$ and σ_X as a function of N_2 , for three different pairs of (κ_1, κ_2) . We choose (5, 45), (15, 35), and (25, 25) partly for convenience and partly for having κ_1 ’s ratios at 1 : 3 : 5.

Focusing on the last pair first (blue points), we note that both curves are symmetric around $N_2 = 100$. Since the simulations were performed for pairs of N_2 around 100, the observed symmetry is an indication of the level of our statistical errors. The values of $\langle X \rangle$ and σ_X at the center are entirely consistent with the findings shown above:

approximately 1300 and 300 respectively. Away from the center, $\langle X \rangle$ appears to decrease slowly at first, but turns up when N_2 reaches to $\sim 10\%$ of the boundaries. The slow decrease is related to $N_1 N_2 = (200 - N_2) N_2$, the maximum allowed value for X . Indeed, in this regime, the fraction

$$f \equiv \langle X \rangle / N_1 N_2 \quad (6)$$

hovers around 13%, i.e., $\sim \kappa\chi$ divided by the average number of nodes in each community. On the other hand, the non-monotonic behavior can hardly be expected. In the next subsection, we will present an approximation scheme which can provide some insight into this remarkable phenomenon.

Turning to the two asymmetric cases, we are not surprised by the lack of symmetry in the curves. However, there are prominent and interesting features, the origins of which do not readily come to mind. First, the levels of $\langle X \rangle$ are generally reduced, despite both χ 's being held at 0.5 and the average preference remaining at 25. Specifically, for a wide range of $N_2 \gtrsim 100$, the f 's are relatively constant, matching roughly the ratio 1 : 3 : 5. Thus, it appears that the introverts are controlling the level of cross-links. Why the extroverts play a lesser role may be argued as follows: When the number of extroverts is well above κ_2 , they can be 'content' by maintaining more links to other extroverts, instead of adding cross-links. Of course, it would be highly desirable to formulate an analytic and more convincing approximation scheme. Second, in addition to the sharp upturn for $N_2 \sim 200$, the peaks of $\langle X \rangle$ are shifted to smaller N_2 , to approximately 20 and 50 for $\kappa_1 = 5$ and 15 respectively. These features can also be roughly argued. Given that the preferred degrees are generally less than the number of nodes, it is understandable that the introverts are more likely to be frustrated, by the eagerness of extroverts to make cross-links. As we decrease N_2 , (especially to values below N_1) we can expect such frustration to decrease, leading to the rise in $\langle X \rangle$ observed. Arguably, an 'optimal' state might be characterized by a balance between the total number of cross-links the introverts prefer, $N_1 \kappa_1$, and that of the extroverts, $N_2 \kappa_2$. (Note that we can ignore χ for this rough argument, since it affects predominantly the *rate* of actions on cross-links). This balance occurs at $N_2 = 4\kappa_1$ for our parameters, i.e., 20 and 60 for the runs with black and red points, respectively. While such arguments produce a rough understanding of the data, more quantitative improvements are clearly needed.

Lastly, we turn to the fluctuations in the cross-links, characterized here by only the standard deviation σ_X , see Fig. 7(b). As pointed out above, these are far larger than naively expected and explaining their presence remains a challenge. Here, we merely highlight what is in the figure: the asymmetric curves for $\kappa_1 \neq \kappa_2$, the variation by over an order of magnitude, and the 'calming influence of the more introverted.' The last of these comments refers to the almost constant σ_X for the $\kappa_1 = 5$ case. We end this subsection with another observation. Noting that the peaks of σ_X for the asymmetric κ 's are also displaced toward the peaks of $\langle X \rangle$, we plot a 'normalized standard deviation,' $\sigma_X / \langle X \rangle$, see inset in Fig. 7(b). It is interesting that the peaks here are now located much closer to the center (though the curves remain asymmetric). Perhaps a detailed analysis of this quantity will facilitate the formulation of a viable theory.

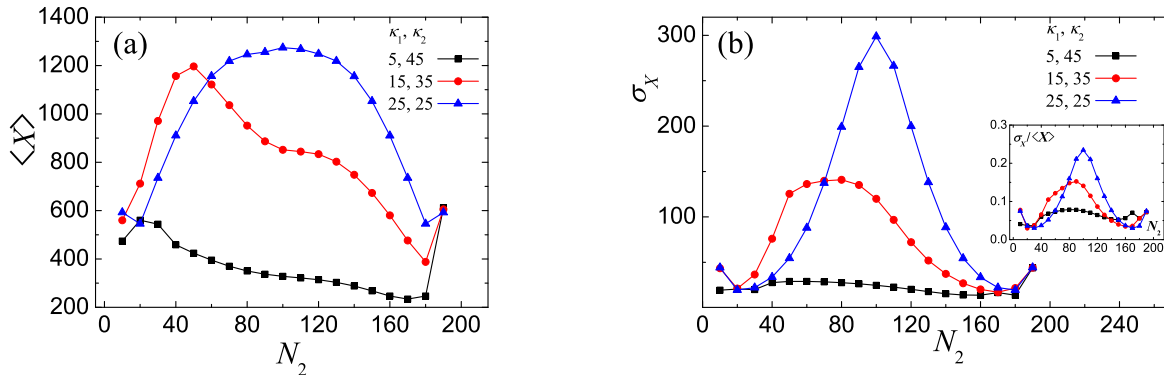


Figure 7. The means (a) and standard deviations (b) associated with cross-links in a two-network model with $\chi_\alpha = 0.5$, $N_1 + N_2 = 200$, $\kappa_1 + \kappa_2 = 50$, as a function of N_2 , for various κ . The inset in (b) shows a plot of $\sigma_X / \langle X \rangle$ versus N_2 .

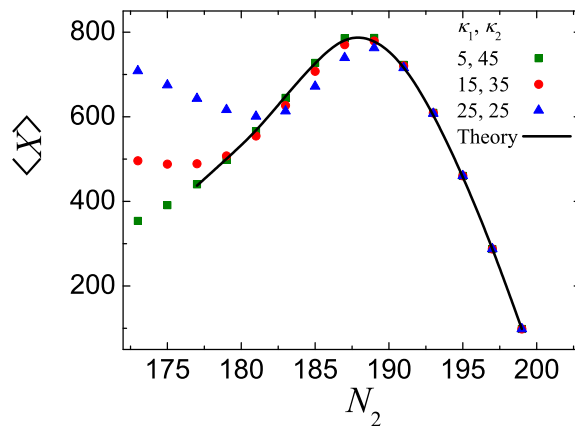


Figure 8. This figure shows $\langle X \rangle$ of systems in the $N_1 \ll N_2$ regime. The associated system parameters are $\chi_\alpha = 0.5$, $N_1 + N_2 = 200$, $\kappa_1 + \kappa_2 = 50$. For this parameter set, the regime with N_2 close to 200 corresponds to the $N_1 \ll N_2$ regime.

3.2.3. Theoretical understanding of X in the $N_1 \ll N_2$ regime. In this last subsection, we present an approximation scheme which provides reasonably good agreement with data in a special regime. It is clear that, in a typical point in parameter space, there are so many competing features in our model that the contributions of all these factors will be difficult to untangle. A remarkable phenomenon – the upturn of $\langle X \rangle$ as N_2 nears its upper bound in Fig. 7(a) – is observed. Moreover, it appears that $\langle X \rangle$ assumes the same value at $N_2 = 190$ for all three pairs of κ 's! It behooves us, therefore, to explore this regime in more detail. The result, shown in Fig. 8, hints at the existence of some underlying ‘universal’ properties. Focusing on this regime, we discover that a simplification emerges, allowing us to gain some insight into this universality.

In the regime of interest, introverts are seriously outnumbered and highly frustrated. In other words, they find themselves with far more contacts than they prefer (i.e.,

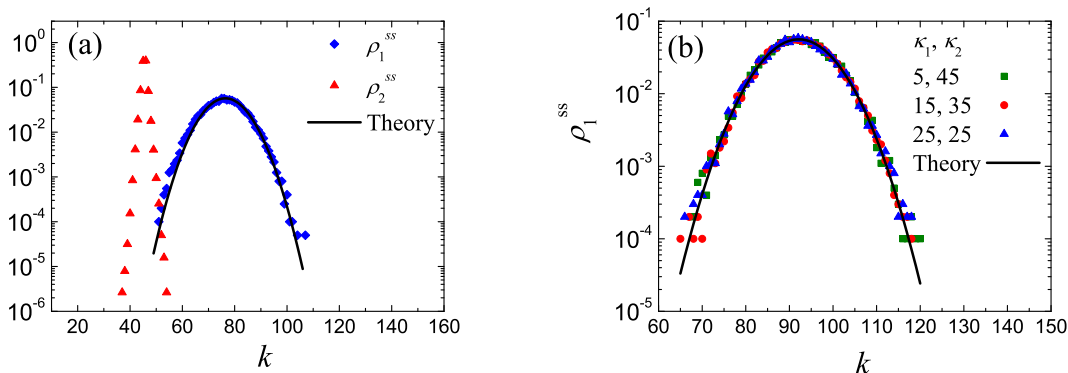


Figure 9. (a) The total degree distributions for a two-network model ($N_1 = 10$, $N_2 = 190$, $\kappa_1 = 5$, $\kappa_2 = 45$ and $\chi_\alpha = 0.5$): ρ_1^{ss} (blue diamonds) and ρ_2^{ss} (red triangles). (b) The total degree distributions ρ_1^{ss} for a two-network model with three different values of κ_1 , κ_2 . The other associated parameters are $N_1 = 5$, $N_2 = 195$, and $\chi_\alpha = 0.5$. In both figures, solid lines represent theoretical predictions.

$k \gg \kappa_1$), so that, when selected to act, they will always cut a link. A more precise and general characterization of this regime is $N_1 \kappa_1 \chi_1 \ll N_2 \kappa_2 \chi_2$. The result of this activity is that there are no (or extremely few) I - I links in the system, so that we can attempt an approximation scheme for $\rho_1^{ss}(k)$, the degree distribution of an I .§ From ρ_1^{ss} , the average $\langle k \rangle$ can be computed. Since every link is a cross-link, $\langle X \rangle$ is just $N_1 \langle k \rangle$.

The strategy here is the same as the one used for the single network: finding the steady state ρ^{ss} by balancing the rates for increasing and decreasing k , namely,

$$\rho^{ss}(k)W[k \rightarrow k+1] = \rho^{ss}(k+1)W[k+1 \rightarrow k] \quad (7)$$

where $W[k \rightarrow k']$ specifies the probability for a node with degree k to become k' . To find the appropriate W 's here, we rely on the following argument. Focus on a particular introvert, i , with existing degree k . For the regime of interest, we can assume $k > \kappa_1$, so that the only way for it to gain a link is for an extrovert (not already connected to i) choosing to add a cross-link to it. Several factors contribute to the rate for such a process:

- $(N_2 - k)/N$, the probability for an extrovert *not* connected to i to be selected
- w_2^+ , the probability that this extrovert will add a link
- χ_2 , the probability for it to add a cross-link (1/2 here), and
- p , the probability that this cross-link is added to i .

Now, in this regime, we believe the extroverts should be mostly ‘content’ ($\kappa_2 \ll N$). This belief is supported by the observed degree distributions, a typical case shown as red points in Fig. 9(a). Thus, we will approximate w_2^+ by 1/2. As for the last quantity,

§ Note that, since we have assumed $k_{11} = 0$, we can drop the subscripts in k_{12} , while $\rho_{12}(k)$ is also identical to $\rho_1(k)$.

p^{-1} should be the number of introverts unconnected to our extrovert. We may estimate it by $N_1(1-f)$, where f is the fraction of cross-links that are present. To be slightly more accurate, especially crucial for small N_1 , we recognize that our extrovert is already connected to i and so, we propose

$$\frac{1}{p} \simeq 1 + (N_1 - 1)(1 - f). \quad (8)$$

Putting the factors together, we have

$$W[k \rightarrow k + 1] = \frac{N_2 - k}{N} w_2^+ \chi_2 p \simeq \frac{(N_2 - k)/4N}{1 + (N_1 - 1)(1 - f)}. \quad (9)$$

On the other hand, the contributions to $W[k + 1 \rightarrow k]$ come from two processes. One is node i being selected to cut a cross-link. The probability of selecting this particular node i is $1/N$, and with rate 1 it will cut a link. But this action will be taken on a cross-link only with probability χ_1 ($1/2$ here). In the other process, an extrovert connected to i is chosen (probability k/N) and cuts one of its cross-links (probability $w_2^- \chi_2 \simeq 1/4$). Following the argument above for p^{-1} , we have

$$\frac{1}{p} \simeq 1 + (N_1 - 1)f. \quad (10)$$

Of course, here p corresponds to the probability that the extrovert *cuts* the cross-link to i . Therefore, we reach at

$$W[k + 1 \rightarrow k] = \frac{1}{2N} + \frac{k + 1}{N} w_2^- \chi_2 p \simeq \frac{1}{2N} + \frac{(k + 1)/4N}{1 + (N_1 - 1)f}. \quad (11)$$

With explicit expressions for the W 's, we exploit Eqn. (7) to derive a recursion relation for the steady state degree distribution:

$$\rho_1^{ss}(k + 1) = \rho_1^{ss}(k) R(k) \quad (12)$$

where

$$R(k) = \left\{ \frac{N_2 - k}{1 + (N_1 - 1)(1 - f)} \right\} \left\{ 2 + \frac{k + 1}{1 + (N_1 - 1)f} \right\}^{-1} \quad (13)$$

Thus, $\rho_1^{ss}(k)$ is explicitly

$$\rho_1^{ss}(k) = \rho_1^{ss}(0) \prod_{\ell=0}^{k-1} R(\ell) \quad (14)$$

where $\rho_1^{ss}(0)$ can be fixed by the normalization $\sum_0^{N_2} \rho_1^{ss}(k) = 1$.

So far, f is not a known quantity. But it can be determined self consistently, through the equations

$$f = \frac{\langle X \rangle}{N_1 N_2} = \frac{\langle k \rangle}{N_2} = \frac{1}{N_2} \sum_0^{N_2} k \rho_1^{ss}(k) \quad (15)$$

The result is a *prediction* (i.e., no fitting parameters) for ρ_1^{ss} and so, $\langle X \rangle$. Plotted as black lines in Figs. 9 and 8, these predictions agree remarkably well – provided we remain in the $N_1 \ll N_2$ regime. Clearly, the deviations of $\langle X \rangle$ from the theoretical curve in Fig. 8 reflect the limits of this regime.

Finally, we return the issue of ‘universality.’ Note that results Eqns. (13,14,15) are *independent* of the κ ’s. Of course, their validity relies on the assumption that $\langle k_1 \rangle \gg \kappa_1$, which seems reasonable in these cases where all the introverts are highly frustrated. In Figs. 9(b), we show data for a more extreme system ($N_1, N_2 = 5, 195$) in which this notion of universality is indeed well borne out. An alternative perspective is that, in this regime, the $N_1 \times N_1$ block of the full $N \times N$ adjacency matrix is frozen at zero, so that much of what we wish to compute can be gleaned from the smaller $N_1 \times N_2$ incidence matrix. As long as we restrict ourselves to considering ‘zero $N_1 \times N_1$ blocks,’ the role of κ_1 is entirely marginal.

4. SUMMARY AND OUTLOOK

In this paper, we present further explorations of preferred degree networks and their interactions in a more systematic Monte Carlo study. Specifically, we consider the effects of just one way of coupling the two networks, through χ , the probability that a node in one network adds or cuts a link to a partner in the other community. Thus, $\chi = 0$ corresponds to two completely decoupled networks, while a system with $\chi = 1$ can be regarded as ‘maximally coupled.’ Even restricting ourselves to this simple interaction, we are faced with a large, 6-dimensional parameter space: the number of nodes in each network ($N_{1,2}$), their preferred degrees ($\kappa_{1,2}$), and their couplings $\chi_{1,2}$. We began with a study of the most symmetric system Eqn. (3), consisting of two *identical* networks coupled by $\chi = 1/2$. With limited computational resources, we ventured from this point onto several 1-d and 2-d subspaces. Here, the preferred degrees are typically different and we chose the convention $\kappa_1 \leq \kappa_2$, referring to them as ‘introverts’ and ‘extroverts.’ Simulating these systems and letting them settle into steady states, we characterize them by measuring various degree distributions as well as the behavior of X , the total number of cross-links between the communities. While some results are expected, other properties are quite surprising.

One remarkable result is the drastically different behavior between two very similar systems, one being the completely symmetric two-network system Eqn. (3) and the other being a single homogeneous network (with the same total population) partitioned into identical halves. In particular, defining X for the homogeneous network as the links between these two halves, we find that its stationary distribution, $P^{ss}(X)$, is well described by a Gaussian distribution, with an easily predicted mean, $\langle X \rangle$, and standard deviation, σ_X . However, in simulations of the symmetric two-network system, $P^{ss}(X)$ displays a very broad and flat plateau. The standard deviation here is an order of magnitude larger and so far, understanding it remains a challenge. The different behaviors indicate that, despite its simplicity, this way of coupling two networks has a

profound effect on the system.

Away from the symmetric systems, most features of the simulation results for $\langle X \rangle$ and σ_X can be qualitatively understood, although a good theory will be needed to provide acceptable quantitative agreements. Remarkably, within the regions we explored, we observed ‘universal’ behavior in asymmetric systems when the introverts are far outnumbered, in the following sense. Not only $\langle X \rangle$ and σ_X , but also the full degree distribution for the introverts, become *independent* of the κ ’s. Insight to this behavior can be found by noting that, in this regime, the introverts are so frustrated that their only action is cutting links. As a result, there are no links between the introverts and the state of each can be specified by the number of cross-links alone. An approximation scheme for their degree distribution can be formulated, leading to very successful predictions.

These findings, though in a rather limited region of control parameter space, reveal many non-trivial phenomena in a system with just two networks, coupled in a simple way. Quantitative explanations of much of the data are still lacking. To make progress, we may extend the same approximation schemes to study the joint distributions $P_\alpha(k_{\alpha\alpha}, k_{\alpha\beta})$. Preliminary analysis indicates that, unlike the exact transition rates for the full, microscopic distribution, such a set of approximate rates obeys ‘local’ detailed balance, i.e., the only irreversible Kolmogorov loops are those around the $k = \kappa_\alpha$ line. Thus, it may be possible for P_α^{ss} to be found analytically. An in-depth study is underway. Meanwhile, along the lines of our successful theory for the special regime here (where the introverts are highly frustrated), we can consider the case in which both parties are ‘maximally frustrated.’ With extreme introverts ($\kappa_1 = 0$) and extroverts ($\kappa_2 = \infty$) in our system, we coined it the ‘XIE model.’ Within a short time, the intra-community links will be frozen (empty and full, respectively) while only the cross-links are dynamic. The $N \times N$ adjacency matrix reduces fully to the $N_1 \times N_2$ incidence matrix and our problem simplifies considerably. Even in this extreme case, surprising behavior emerges, some of which has been reported [24]. Thanks to the restoration of detailed balance, we can solve the master equation and find the microscopic stationary distribution exactly [24]. The next paper of this series [26] will be devoted to more systematic simulations as well as more in-depth analytic studies.

Acknowledgments

We thank K. Bassler, S. Jolad, L.B. Shaw and Z. Toroczkai for illuminating discussions. This research is supported in part by the US National Science Foundation, through grant DMR-1244666.

References

- [1] Liu W, Jolad S, Schmittmann B and Zia R K P 2013 *J. Stat. Mech. Theory Exp.* **2013** P08001
- [2] Strogatz S H 2001 *Nature* **410** 268
- [3] Albert R and Barabási A-L 2002 *Rev. Mod. Phys.* **74** 47

- [4] Dorogovtsev S N and Mendes J F F 2002 *Adv. Phys.* **51** 1079
- [5] Newman M E J 2003 *SIAM Rev.* **45** 167
- [6] Estrada E, Fox M, Higham D and Oppo G-L (eds) 2010 *Network Science: Complexity in Nature and Technology* (Springer, New York)
- [7] Watts D J and Strogatz S H 1998 *Nature (London)* **393** 440
- [8] Albert R, Jeong H and Barabási A-L 1999 *Nature (London)* **401** 130
- [9] Barabási A-L and Albert R 1999 *Science* **286** 509
- [10] Barrat A, Barthélemy M and Vespignani A 2008 *Dynamical processes on complex networks* (Cambridge University Press)
- [11] Dorogovtsev S N, Goltsev A V and Mendes J F F 2008 *Rev. Mod. Phys.* **80** 1275
- [12] Gross T, D’Lima C J D and Blasius B 2006 *Phys. Rev. Lett.* **96** 208701
- [13] Gross T and Blasius B 2008 *J. R. Soc. Interface* **5** 259
- [14] Rinaldi S, Peerenboom J and Kelly T 2001 *IEEE Contr. Syst. Mag.* **21** 11
- [15] Panzieri S and Setola R 2008 *Int. J. Model. Ident. Contr.* **3** 69
- [16] Vespignani A 2010 *Nature (London)* **464** 984
- [17] Buldyrev S V, Parshani R, Paul G, Stanley H E and Havlin S 2010 *Nature (London)* **464** 1025
- [18] Buldyrev S V, Shere N W and Cwilich G A 2011 *Phys. Rev. E* **83** 016112
- [19] Kurant M and Thiran P 2006 *Phys. Rev. Lett.* **96** 138701
- [20] Erdős P and Rényi A 1959 *Pub. Math.* **6** 290
- [21] Platini T and Zia R K P 2010 *J. Stat. Mech. Theory Exp.* **2010** P10018
- [22] Zia R K P, Liu W, Jolad S and Schmittmann B 2011 *Physics Procedia* **15** 102
- [23] Jolad S, Liu W, Schmittmann B and Zia R K P 2012 *PLoS ONE* **7(11)** e48686
- [24] Liu W, Schmittmann B and Zia R K P 2012 *EPL* **100** 66007
- [25] Zia R K P and Schmittmann B 2007 *J. Stat. Mech. Theory Exp.* **2007** P07012
- [26] Liu W, Bassler K E, Schmittmann B, and Zia R K P to be published.